

The Kinetics of Adsorption of CO on Group VIII Transition Metals¹

Chemisorption, the binding of an adsorbate molecule to a substrate, is one of the elementary chemical reactions which occurs in all more complex heterogeneously catalyzed reaction mechanisms. Thus, it is of fundamental importance to understand the kinetics of adsorption in order to describe surface reaction mechanisms quantitatively. In this note, we examine the kinetics of adsorption of CO on the Group VIII transition metals Ni, Ru, Pd, Ir and Pt. All experimental results are characteristic of adsorption on atomically clean single crystal surfaces, and, in addition, we consider two different geometries of the Pt surface. Thus, we are able to assess both the effect of electronic structure upon adsorption kinetics, as we vary the transition metal substrate, and the effect of geometric structure, as we examine the two different Pt surfaces.

The rate of adsorption onto a solid surface may be written as

$$R_a = (p/(2\pi MkT)^{1/2})S(\theta) = C_s(d\theta/dt), \quad (1)$$

where p is the pressure, M is the adsorbate mass, k is the Boltzmann constant, T is the absolute temperature, $S(\theta)$ is the probability of adsorption on the surface which is a function of the fractional surface coverage θ , C_s is the two-dimensional concentration of adsorption sites, and t is

¹ Work supported by the North Atlantic Treaty Organization under Grant No. 898; and by the Donors of the Petroleum Research Fund, administered by the American Chemical Society (WHW).

² To whom all correspondence should be sent.

time. It should be noted that $p/(2\pi MkT)^{1/2}$ is the gas flux onto the surface, and the rate of Eq. (1) is written in units of flux.

A convenient independent variable to use when discussing adsorption is the *exposure* of gas to the surface where the exposure ϵ is defined to be the product of pressure and time. If we further define $(2\pi MkT)^{1/2} \equiv \kappa$, then Eq. (1) may be rewritten as

$$d\theta/d\epsilon = S(\theta)/\kappa C_s. \quad (2)$$

Thus, if data exist which relate the fractional surface coverage to the gas exposure, it is possible to test alternate models concerning the adsorption kinetics, i.e., to deduce the functional relationship for $S(\theta)$.

For example, in the Langmuir model of adsorption,

$$S(\theta) = S_0(1 - \theta), \quad (3)$$

where S_0 is the probability of adsorption in the limit of zero surface coverage. This model assumes that the adsorption kinetics are first order with respect to the fraction of vacant sites. If the adsorption were second order in the fraction of vacant sites, as would occur for example were the adsorption dissociative or if the initial adsorbate-substrate bond formation depended on two adjacent vacant sites as a result of the microscopic nature of inter-adsorbate vs adsorbate-substrate interactions, then we would have

$$S(\theta) = S_0(1 - \theta)^2. \quad (4)$$

Kisliuk (1, 2) has considered an adsorption model which includes the possibility

that the adsorbate is trapped at the surface in a "precursor" state which may be thought of as a physically adsorbed state. The fundamental idea in this model is that an adsorbate which is initially located above another adsorbate molecule may diffuse across the surface until it encounters a vacant adsite onto which it may then chemisorb. Based on this model, Kisliuk (1) was able to derive the following expression for $S(\theta)$

$$S(\theta) = S_0\{(1 - \theta)/(1 - c\theta)\} \quad (5)$$

for molecular (associative) adsorption. In Eq. (5), the parameter c is given by (1)

$$c = (P_a + P_b - P_b')/(P_a + P_b), \quad (6)$$

where P_a is the probability of adsorption of the precursor molecule on an empty substrate site, P_b is the probability of desorption of the precursor from an empty site, and P_b' is the probability of desorption of the precursor from a filled site. Thus, we see that for $c = 0$, we retrieve the Langmuir model since $P_a + P_b = P_b'$. Moreover, for $c > 0$, we have the case where the physically adsorbed molecule can remain on the surface a relatively long time until it encounters an adsite. In the limit of $c = 1$, we have the case of a constant adsorption probability up to saturation coverage. This corresponds to an effectively infinite precursor state lifetime. On the other hand, if $c < 0$, then the adsorption probability falls off even more rapidly than the Langmuir model.

The integrated rate expression assuming the Langmuir (first-order) model of Eq. (3) is given by

$$-\ln(1 - \theta) = (S_0/\kappa C_s)\epsilon \quad (7)$$

assuming second-order kinetics as indicated in Eq. (4) is given by

$$\theta/(1 - \theta) = (S_0/\kappa C_s)\epsilon, \quad (8)$$

and assuming the Kisliuk precursor model

of Eq. (5) is given by

$$\begin{aligned} f(\theta) &\equiv c\theta - (1 - c) \ln(1 - \theta) \\ &= (S_0/\kappa C_s)\epsilon. \end{aligned} \quad (9)$$

We will now apply the formalism of Eq. (7)–(9) to CO chemisorption on various Group VIII transition metal surfaces. This is a particularly convenient choice for three reasons: (i) The adsorption is reversible and associative so that effects due to the surface disproportionation of the CO need not be considered; (ii) the Group VIII transition metals are efficient oxidation catalysts so it is a useful exercise to consider the detailed chemisorption mechanism; and (iii) the necessary experimental data obtained under controlled ultrahigh vacuum (UHV) conditions using low-energy electron diffraction (LEED), thermal desorption mass spectrometry, and contact potential difference measurements are available for CO chemisorption on (111) Ni (3), (001) Ru (4), (111) Pd (5), (111) Ir (6), and both (111) and (110) Pt (7,8). All of these surfaces, with the exception of the (110) Pt, are hexagonally close-packed in two dimensions so we can judge primarily electronic structural effects in the chemisorption by maintaining a constant geometrical structure. Moreover, we examine both the (111) and (110) surfaces of Pt in order to distinguish geometrical effects on substrates with the same bulk electronic structure.

We summarize our results in Table 1. In this table, we show the kinetic model which fits the chemisorption data. the value of the initial probability of adsorption. the surface structures observed in LEED, the adsorbate concentration corresponding to the various ordered overlayer structures, and the isosteric heat of adsorption in the limit of low surface coverage. The first thing to note in Table 1 is the form of the adsorption probability, $S(\theta)/S_0$, on the various metal surfaces. The adsorption of CO on the (111) sur-

TABLE 1
Parameters Pertaining to the Chemisorption of CO on Various Group VIII
Transition Metal Surfaces

Substrate	$S(\theta)/S_0$	S_0	Surface structure	Adsorbate concentrations (cm ⁻²)	Isosteric heat of adsorption (kcal/mol) at low coverage	References
Ni (111)	$\frac{1-\theta}{1-0.4\theta}$	0.97	($\sqrt{3} \times \sqrt{3}$)R30° Compressed ($\sqrt{3} \times \sqrt{3}$)R30°	6.2×10^{14} 1.0×10^{15}	26.5	(3)
Ru (001)	$\frac{1-\theta}{1-0.35\theta}$	0.57	($\sqrt{3} \times \sqrt{3}$)R30° ($2\sqrt{3} \times 2\sqrt{3}$)R30°	5.2×10^{14} 9.1×10^{14}	29	(4)
Pd (111)	$\frac{1-\theta}{1-0.5\theta}$	1.75	($\sqrt{3} \times \sqrt{3}$)R30° Compressed ($\sqrt{3} \times \sqrt{3}$)R30°	5.1×10^{14} 7.7×10^{14}	34	(5)
Ir (111)	$(1-\theta)^2$	1.10	($\sqrt{3} \times \sqrt{3}$)R30° ($2\sqrt{3} \times 2\sqrt{3}$)R30°	5.2×10^{14} 9.1×10^{14}	35	(6)
Pt (111)	$\frac{1-\theta}{1-0.85\theta}$	0.52	No ordered structures	7.7×10^{14} (at saturation)	30	(7)
Pt (110)	$\frac{1-\theta}{1-0.88\theta}$	1.10	<i>p1g1</i> (2×1)	9.2×10^{14}	32	(7, 8)

faces of Ni, Pd, and Pt, the (001) basal plane of Ru, and the (110) surface of Pt all follow a precursor state mechanism although with rather different values of the parameter c [compare Eq. (5) and (6)]. On the other hand, the CO adsorption on the Ir (111) surface follows second-order kinetics with respect to the fraction of vacant surface sites. As may be seen from Eq. (9), a plot of $c\theta - (1-c) \times \ln(1-\theta)$ as a function of ϵ should be linear if the precursor model is a correct representation of the data, and the slope of the resulting line yields the initial probability of adsorption, S_0 . The appropriate plots for Ni, Ru, Pd and both surfaces of Pt are shown in Fig. 1, and it is clear a precursor model is followed in all these cases. The values of the parameter c which linearize the data are correct to within approximately ± 0.05 . Thus,

although the kinetics of adsorption on (111) Ni, (001) Ru, and (111) Pd are quite similar, they are certainly different from those observed on both (111) and (110) Pt. The larger value of c on Pt means that the effective residence time on the Pt surfaces are longer than on the Ni, Ru, and Pd.

The CO chemisorption on (111) Ir follows second-order kinetics, i.e., the adsorption rate is proportional to $(1-\theta)^2$, as may be seen from the linear relationship between $\theta/(1-\theta)$ and ϵ in Fig. 1 [compare Eq. (8)]. All attempts to fit the (111) Ir data to a precursor model were unsuccessful. We thus conclude both that the surface residence time of the CO on the Ir is quite short, i.e., the vibrational energy exchange between the molecule and the surface is inefficient, and also that a pair of adjacent vacant sites are required

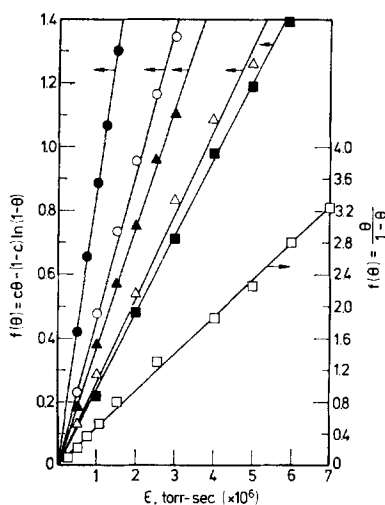


Fig. 1. Demonstration that the Kisliuk precursor model is appropriate for CO adsorption on (111) Ni, (001) Ru, (111) Pd, (111) Pt, and (110) Pt, whereas second-order adsorption kinetics apply for CO on (111) Ir. (●), Pd (111); (○), Pt (110); (▲), Ni (111); (△), Pt (111); (■), Ru (001); (□), Ir (111).

for CO adsorption on Ir. It is interesting to note that CO chemisorption does not obey Langmuir kinetics [see Eq. (7)] on any of the Group VIII transition metals examined.

The initial probability of adsorption may be determined from the slopes of Fig. 1 as indicated in Eq. (8) and (9), and the values of S_0 so determined are shown in Table 1. We see that the initial probability of adsorption on Ni (111), Ir (111), and Pt (110) is essentially unity, whereas it is approximately 0.5 on both Ru (001) and Pt (111). The abnormally large value of S_0 on Pd (111) is attributed to a gauge calibration error, and we believe that, as on the (111) Ni, (111) Ir, and (110) Pt surfaces, the initial adsorption probability is close to unity on (111) Pd as well.

We also summarize in Table 1 the experimental data pertaining both to the geometry of the CO overlayer as well as the corresponding densities of the adlayer and the initial isosteric heats of adsorp-

tion. As noted previously (6), the similarities are striking. On all the hexagonal close-packed surfaces with the exception of (111) Pt, a $(\sqrt{3} \times \sqrt{3}) R30^\circ$ overlayer is formed at one-third monolayer coverage. At greater coverages, this overlayer is compressed until a $(2\sqrt{3} \times 2\sqrt{3}) R30^\circ$ structure is formed both on Ru (001) and Ir (111). This structure is not seen on Ni (111) due to the small lattice spacing of the Ni (6). It is unclear why it is not formed on (111) Pd; indeed, perhaps it would be if the adsorption were carried out below room temperature. As expected, a different ordered array is observed on (110) Pt since this surface is relatively open and of twofold symmetry, whereas the others are close-packed and of higher symmetry. The saturation surface densities of CO are all quite reasonable varying from 7.7×10^{14} to 1.0×10^{15} cm $^{-2}$ on the six metal surfaces. This corresponds to a molecular diameter ranging from 3.63 to 3.29 Å in the compressed overlayer at saturation coverage. As may be seen in Table 1, the isosteric heats of adsorption are quite similar among all the metal surfaces considered, ranging from 26.5 kcal/mol on Ni (111) to 35 kcal/mol on Ir (111).

Our general conclusion is that CO adsorption on various of the Group VIII transition metal surfaces has a number of similarities and yet some fundamental differences as well. In particular, we have established the following considering both our own data (6-8) as well as previously published data (3-5).

(i) CO adsorption on (111) Ni, (001) Ru, (111) Pd, and both (111) and (110) Pt all obey a kinetic model which assumes that a precursor state is present on the metal surface.

(ii) The residence times of the precursor state on Ni, Ru, and Pd are approximately the same, and they are shorter than the corresponding times on both Pt surfaces.

The residence time on Pt does not vary between the (111) and (110) orientations.

(iii) CO adsorption on Ir is fundamentally different. The kinetics obey a rate law which is second order in vacant surface sites, and the precursor model does not fit the data. This implies that the energy exchange between the CO and the Ir is inefficient and that the presence of an adjacent CO admolecule inhibits the electronic rearrangement required to form the adsorbate-substrate bond.

(iv) The initial probability of adsorption (at zero surface coverage) is approximately unity for CO on (111) Ni, (111) Pd, (111) Ir, and (110) Pt, whereas it is approximately 0.5 on (001) Ru and (111) Pt. Our method of deducing S_0 is based on the entire data set of surface coverage as a function of exposure rather than relying on initial slopes as has often been done in the past.

(v) The CO forms similar ordered overlayers as judged by LEED on the (111) Ni, (001) Ru, (111) Pd, and (111) Ir surfaces. At one-third monolayer coverage, a $(\sqrt{3} \times \sqrt{3}) R30^\circ$ structure is observed, and this compresses at higher coverages forming a $(2\sqrt{3} \times 2\sqrt{3}) R30^\circ$ structure both on Ru (001) and Ir (111). Since all these surfaces are geometrically quite similar, namely hexagonal close-packed, this agreement is not surprising. What is surprising is that no ordered LEED arrays are observed for CO adsorption on (111) Pt under any experimental conditions.

(vi) The saturation density of the adsorbed CO on all the transition metal surfaces is quite similar, varying from $7.7 \times 10^{14} \text{ cm}^{-2}$ on (111) Pd and (111) Pt to $1.0 \times 10^{15} \text{ cm}^{-2}$ on (111) Ni.

(vii) The initial isosteric heats of adsorption on all the Group VIII metals considered are also comparable in magnitude, ranging from 26.5 kcal/mol on (111) Ni to 35 kcal/mol on (111) Ir.

REFERENCES

1. Kisliuk, P. J., *J. Phys. Chem. Solids* **3**, 95 (1957).
2. Kisliuk, P. J., *J. Phys. Chem. Solids* **5**, 78 (1958).
3. Christmann, K., Schober, O. and Ertl, G., *J. Chem. Phys.* **60**, 4719 (1974).
4. Madey, T. E., and Menzel, D., *Jap. J. Appl. Phys. Suppl.* **2**, Part 2, 229 (1974).
5. Ertl, G., and Koch, J. in "Adsorption-Desorption Phenomena" (F. Ricca, Ed.), p. 345. Academic Press, New York, 1972.
6. Comrie, C. M., and Weinberg, W. H., *J. Vac. Sci. Technol.*, Jan./Feb. (1976); *J. Chem. Phys.* **64**, 250 (1976).
7. Comrie, C. M., Ph.D. Thesis, University of Cambridge, Cambridge, 1974.
8. Comrie, C. M., and Lambert, R. M., to be published.

W. H. WEINBERG²

*Division of Chemistry and Chemical Engineering
California Institute of Technology
Pasadena, California 91125*

C. M. COMRIE R. M. LAMBERT

*Department of Physical Chemistry
University of Cambridge
Cambridge CB2 1EP, England
Received September 22, 1975*